

High Efficient Maximum Power Point Tracking for Multiple Solar Strings with GaN-Based HiLEM Circuit

1st Becker Marcus
Elektrotechnisches Institut (ETI)
Karlsruhe Institute of Technology
 Karlsruhe, Germany
 marcus.becker@kit.edu

2nd Stefanski Lukas
Elektrotechnisches Institut (ETI)
Karlsruhe Institute of Technology
 Karlsruhe, Germany
 lukas.stefanski@kit.edu

3rd Hiller Marc
Elektrotechnisches Institut (ETI)
Karlsruhe Institute of Technology
 Karlsruhe, Germany
 marc.hiller@kit.edu

Abstract—This paper discusses the potentials of string based Maximum Power Point Tracking (MPPT) in ground-mounted solar power plants using the HiLEM topology. First, the functionality of the HiLEM circuit is described, then the planned setup with the HiLEM topology is presented. Finally, the operating principle is illustrated by a simulated shading scenario.

Index Terms—Solar energy, Photovoltaic power systems, Maximum Power Point Tracking (MPPT), DC-DC converters

I. INTRODUCTION

Photovoltaic (PV) power plants play a decisive role in the conversion from today’s energy generation to the future based on renewable sources. The government of the Federal Republic of Germany has defined a development path for the expansion of renewable energies in the ”Renewable Energies Act - EEG 2023” [1]. This targets an installed capacity of 215 GW_p for solar energy in 2030 and 400 GW_p for 2040 in Germany. To achieve these goals, it is necessary to build many new plants, but also to increase the efficiency of existing plants through repowering.

Since the consumption of land area in densely populated regions of the world is a major problem, it is necessary to use the available land as efficiently as possible. This is done, for example, through dual-use such as ”Agrivoltaics” or the use of existing roof areas. However, large-scale ground-mounted PV systems also need to be optimized in their use of land.

In current large-scale ground-mounted PV systems, large, powerful, central inverters with several 100 kW to several MW of power are usually used to feed solar energy into the power grid. The systematic structure of a large ground-mounted PV system is often as follows:

Typically, 20 to 35 solar modules are connected in series, up to a system voltage between 1000 V and 1500 V, to form strings. Several of these strings are connected in parallel inside combiner boxes, see Fig. 1. However, this setup has a considerable disadvantage: It is not possible to take the voltage discrepancy of the different strings, caused by mismatch in consideration [2]. Mis-

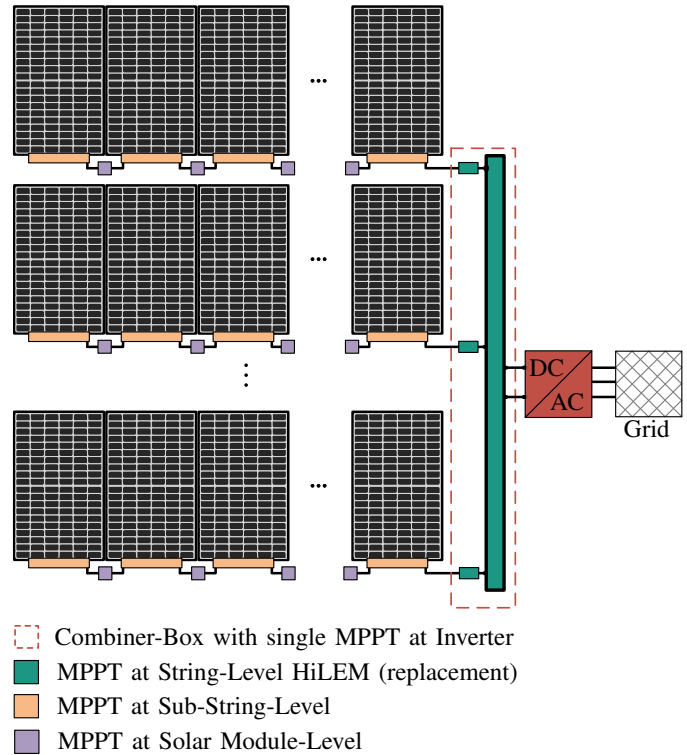


Fig. 1: MPPT Level in large-scale ground-mounted PV systems

match refers to the power loss, caused by differences in irradiation, shading, soiling, aging, orientation, tilt or solar module types in the individual strings. Since the central inverter has only one DC voltage input, it can only set a single Maximum Power Point (MPP) voltage for all strings together. Therefore, strings with a deviating MPP voltage are not operated optimally, which leads to a reduction in the energy yield of the entire system.

Individual MPPT of each string is possible by adding multiple boost converters, electrically isolated converters or other topologies [3] to the strings. But they all result in higher costs and increased losses, if no mismatch is present at the moment. Actually, these technologies are used in conventional string inverters, with a power range of 2 kW to 200 kW, but due to economical reasons not in large central inverters. Recently, the request for string based MPPT is increasing in these type of systems, for this reason string inverters are being used more and more in large ground-mounted PV systems. Therefore, research interest in more efficient and cost-effective solutions for string based MPPT is currently increasing.

In this paper the further development and setup of the High Efficiency Low Effort MPPT (HiLEM) [4] circuit in a PV research plant is presented. The purpose of this research plant is to investigate the efficiency gained through the HiLEM circuit with MPPT at string level on a ground-mounted PV system. As a reference, combiner boxes as well as conventional string inverters will be compared in terms of their overall efficiency.

In Section II the HiLEM circuit is presented. The hardware setup of the HiLEM system is described in Section III and the simulation results of a potential shading scenario are presented in Section IV.

II. HiLEM CIRCUIT FOR ULTRA EFFICIENT MPPT

First introduced in [5], the HiLEM circuit provides a highly efficient method to operate multiple strings of a PV system at their individual MPP. The circuit exploits the circumstance that it is not necessary to have a voltage range at the converter input down to 0 V for a reasonable operation. Furthermore, an input voltage range between the lowest string voltage $u_{G,\min}$ and the highest string voltage $u_{G,\max}$ is sufficient to operate all strings in their MPP. This is evident from the power curves shown in Fig. 2.

The patented HiLEM circuit described in [4], [5] and shown in Fig. 3 reduces the switched voltages to $u_{G,\text{diff}} = u_{G,\max} - u_{G,\min}$. For this reason, semiconductors with a lower blocking voltage can be used compared to, for example, a boost converter topology. This leads to

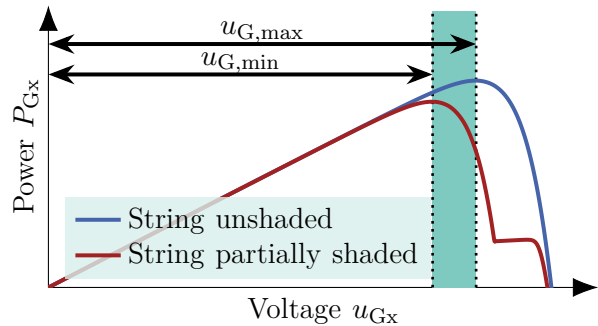


Fig. 2: Difference in power and voltage between unshaded and partially shaded strings; Parameters from Table 2 of [6]

very low losses also at higher switching frequencies, allowing smaller passive components to be used compared to conventional full power DC-DC converters [7]. This further reinforces the advantages mentioned above. There are several versions of the HiLEM circuit as described in [4]. For the setup of the PV research plant, only the HiLEM-2 version is of interest and will be abbreviated as HiLEM in this paper.

Each of the N PV strings has its own input half-bridge in the HiLEM circuit configuration shown in Fig. 3 on the left side. These consist mainly of the two semiconductors $T1x$ and $T2x$, the capacitors $C4x$ and the inductors $L1x$ with $x \in \{1 \dots N\}$. The N input side half-bridges are connected by $W1$, $W2$ and $W3$ and combined by the single output side half-bridge to a common DC output. The HiLEM output half-bridge consists of the two semiconductors $T3$ and $T4$, the capacitor $C3$ and the inductor $L2$. The split DC link is formed by capacitor $C1$ between $W1$ and $W2$ and capacitor $C2$ between $W2$ and $W3$.

The MPP voltage u_{Gx} for the individual PV strings can be adjusted in the range between $u_{C2} \leq u_{Gx} \leq u_{C2} + u_{C1}$. Within certain limits, caused by the blocking voltage of the semiconductors, the voltage level for u_{C1} and u_{C2} can be varied. If u_{C1} is chosen as small as possible and u_{C2} as large as possible, the switching losses in the switched semiconductors can be minimized [4]. The circuit provides a DC voltage u_A between terminal A+ and A-, to which a grid feeding inverter can be connected. Neglecting all losses, the mean value of the output voltage u_A is always between $u_{G,\min}$ and $u_{G,\max}$.

Pulse width modulation (PWM) is used to control the transistors $T1x$ - $T4$. The duty cycle of the input half-bridges are designated as a_{Dx} and those of the output half-bridge as a_F . With the switching frequency f_{SW} ,

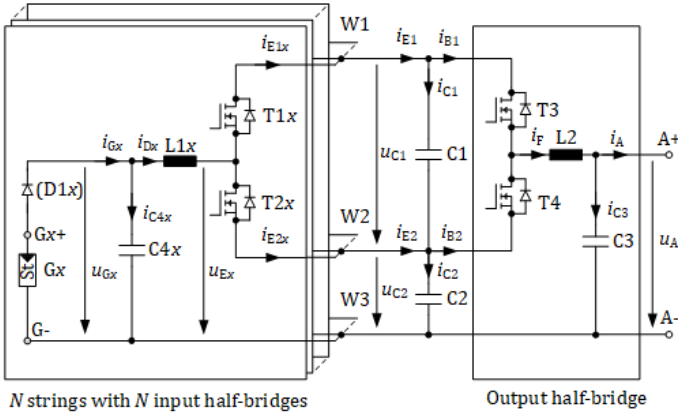


Fig. 3: HiLEM-2 circuit [7]

the length of the power-on periods

$$T_{T1x} = a_{Dx} \cdot \frac{1}{f_{sw}} \quad (1)$$

$$T_{T2x} = (1 - a_{Dx}) \cdot \frac{1}{f_{sw}} \quad (2)$$

$$T_{T3} = a_F \cdot \frac{1}{f_{sw}} \quad (3)$$

$$T_{T4} = (1 - a_F) \cdot \frac{1}{f_{sw}} \quad (4)$$

result [7]. For the stationary mode the current i_{C4x} can be neglected resulting in $i_{Gx} \approx i_{Dx}$. T1x and T2x split the input current i_{Dx} of the input half-bridge into the currents i_{E1x} and i_{E2x} . According to [7], the two mean values during one pulse-period result as:

$$\bar{i}_{E1x} = a_{Dx} \cdot i_{Gx} \quad (5)$$

$$\bar{i}_{E2x} = (1 - a_{Dx}) \cdot i_{Gx} \quad (6)$$

The two currents i_{B1} and i_{B2} are combined by the transistors T3 and T4 of the output half-bridge to form the current i_F .

Modeling the N input half-bridges as one equal input half-bridge simplifies the circuit. The sum of all input currents i_{Gx} results in the equivalent input current i_G and the sum of all inductor currents i_{Dx} result in the equivalent current i_D [7]:

$$i_G = \sum_{x=1}^N i_{Gx} \quad (7)$$

$$i_D = \sum_{x=1}^N i_{Dx} \quad (8)$$

Assuming that all individual powers $P_{Gx} = u_{Gx} \cdot i_{Gx}$ are summed to the equivalent power $P_G = u_G \cdot i_G$, the result for the equivalent voltage u_G is:

$$u_G = \frac{P_G}{i_G} = \frac{\sum_{x=1}^N u_{Gx} \cdot i_{Gx}}{i_G} \quad (9)$$

If the losses of the circuit are neglected, then in stationary operation, where no capacitor is charged or discharged, the input power $P_G = u_G \cdot i_G$ is equal to the output power $\bar{P}_F = u_A \cdot \bar{i}_F$. Thus, the output current i_A is equal to the equivalent input current i_G respectively equal to \bar{i}_F and \bar{i}_D and thus $u_A \approx u_G$.

$$i_A = \bar{i}_F = \bar{i}_D = i_G \quad | \quad u_A \approx u_G \quad (10)$$

It follows from the topology that the output voltage u_A is in the range between $u_{G,\min}$ and $u_{G,\max}$. Therefore, it is not possible to boost the output voltage u_A above the value of $u_{G,\max}$. Usually this is not necessary, because most inverters can be operated with different DC voltages and the minimum voltage for feeding into the grid is ensured by the setup of the entire PV system, i.e., the number and the type of the solar modules.

One advantage of the HiLEM circuit is the reduced total switching power compared to a conventional full power circuit with one boost converter for each of the N PV strings. The switching power is the sum of the products of the drain-source voltage and the drain current from each of the four transistors. The current i_{Gx} is the maximum possible current of the PV strings and the voltage u_{C1} is the difference between $u_{G,\max}$ and $u_{G,\min}$. This yields the total switched power of the HiLEM circuit [7]

$$P_{sw,HiLEM} = N \cdot 4 \cdot (u_{G,\max} - u_{G,\min}) \cdot i_{G,\max} \quad (11)$$

For a conventional boost converter, the total switched power results to

$$P_{sw,boost} = N \cdot 2 \cdot u_{G,\max} \cdot i_{G,\max} \quad (12)$$

A low total switching power leads to low losses and therefore a higher efficiency. From Eq. 11 and Eq. 12 it is obtained, that as long as the difference $u_{G,\max} - u_{G,\min}$ is less than 50% of $u_{G,\max}$, the HiLEM circuit has the lower total switching power resulting in less switching losses.

Since the switching losses, as shown in Eq. 11 are directly proportional to the voltage $u_{C1} = u_{G,\max} - u_{G,\min}$, the voltage u_{C1} is kept at the lowest possible value $u_{G,\max} - u_{G,\min}$ during operation. Since the smallest and largest string voltage change dynamically during operation due to the MPPT, a dynamic adjustment of the voltage u_{C1} is possible and will have significant effects on the overall efficiency. So far, only setups of the HiLEM circuit with a fixed voltage u_{C1} are investigated [4], [7].

Because of the low maximum value of the voltage u_{C1} , the semiconductors T1x – T4 and the capacitor

C1 can be designed for considerably lower voltage than the maximum string voltage. Therefore, Gallium Nitride (GaN) transistors are particularly suitable for use within HiLEM, since they have a low $R_{DS(on)}$, allow very high switching frequencies and the topology does not require high blocking voltages. As a result, the passive components of the circuit can be dimensioned smaller, leading to a further cost reduction. For reasons of limited space and since this paper focuses on the overall system, we refer to [4], [7] for a detailed derivation and description of the control scheme of the HiLEM circuit.

III. HARDWARE SETUP OF THE HiLEM SYSTEM

For the application of the HiLEM topology in a dedicated research plant, a consideration of the overall system is made in this section.

The designed HiLEM prototype for the research plant is flexible in use due to its modular design. Up to four HiLEM input stages can be combined with one HiLEM output stage. Each input stage has a power of approximately 10 kW_p and each output stage approximately 40 kW_p . The power rating will also allow the use of very powerful solar modules with up to 500 W_p per module while still being able to utilize the 1000 V system voltage.

A key design feature of the HiLEM circuit is the design of the voltage range of u_{C1} . This determines the required blocking voltage of the semiconductors. It is planned to install solar modules with substring MPP optimizers from a project partner in the research plant. In case of shading of a module, these optimizers act like buck converters. The module voltage is regulated in such a way that the string current i_{Gx} does not change, but the module is still operated in its MPP. As a result, the output voltage of the modules with an optimizer is proportional to the output power when shaded. Therefore, using the substring optimizers, a higher voltage difference between several strings $u_{G,max} - u_{G,min}$ is to be expected, which has to be taken into account in the design of the HiLEM prototype.

As described in Section II, the HiLEM topology has efficiency benefits as long as $u_{G,max} - u_{G,min}$ does not exceed 50% of $u_{G,max}$. Since the MPP voltage of one string is around 700 V to 800 V , a maximum voltage for u_{C1} of 400 V is set.

For the prototype of the HiLEM input stage the GaN transistors (GS66508T) [11] from *GaN Systems* with a blocking voltage of 650 V and a maximum drain-source current of 30 A are used. The output stage is still in the design process, will also be equipped with GaN transistors (GS66516T) [12] from *GaN Systems*

with 650 V blocking voltage, but with a maximum drain-source current of 60 A .

Since the overall system is presented in this paper, the further hardware structure of the prototypes will not be discussed in depth at this point. The detailed design with measurements on the hardware will be presented in a following publication.

The research plant for the HiLEM circuit will consist of a total of eight strings, each with 21 solar modules. Four strings will be connected to the HiLEM system and the other four strings will be connected conventionally

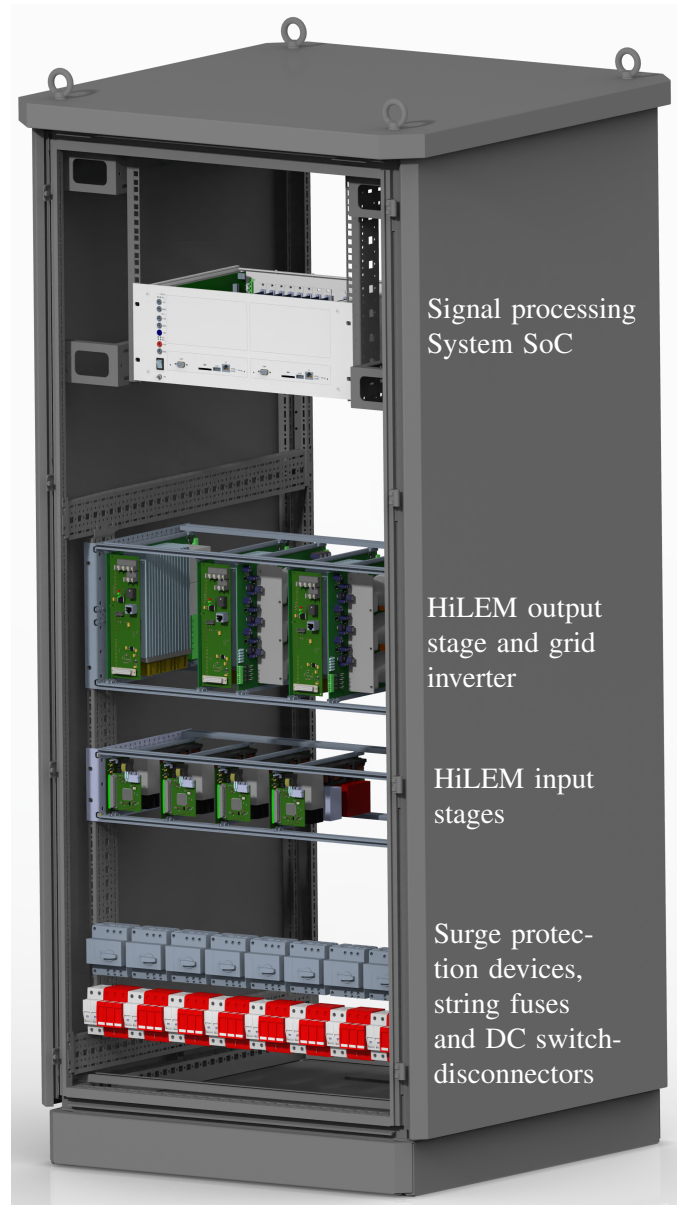


Fig. 4: CAD model of the planned setup of the HiLEM circuit in the outdoor cabinet

with a combiner box and are used as a reference for validation.

The hardware of the HiLEM circuit for the research plant is to be housed in an outdoor cabinet. An illustration of the provisional CAD model can be seen in Fig. 4. On the lowest level, the eight incoming strings are connected to surge protection devices, string fuses and DC switch-disconnectors. This way, the strings can be flexibly distributed between the subsystem with the HiLEM circuit and the subsystem of the reference plant. The DC switch-disconnectors are either switched manually or are automatically switched off for safety reasons when the grid is disconnected. It is also possible to turn off the switches by the signal processing system in the case of a detected fault. On the middle level are the racks for the power electronic hardware of the HiLEM topology. The input stages are designed in the *Eurocard* format 100 mm x 280 mm seen on the lower rack. The output stage has a double *Eurocard* format 230 mm x 280 mm seen on the upper rack. Grid feeding inverter with the same format, are also placed on this level. The inverter developed in-house provides full access to all relevant parameters necessary for research purposes [9]. The signal processing in the upper area shown in Fig. 4 is primarily used for research tasks. The signal processing system is mainly based on a Xilinx Zynq 7030 System on Chip (SoC). On a single chip, it combines an Field Programmable Gate Array (FPGA) with a dual core ARM processor chip [10]. Communication between the SoC and the individual HiLEM stages is enabled by optical fibers. This allows the SoC system to be used for high-performance measurement recording in the research plant.

The HiLEM circuit can be operated completely independently, since each input stage as well as the output stage is provided with its own Local Control Unit (LCU). This LCU consists mainly of an FPGA of the type Intel® MAX® 10 10M08 or 10M25 for the output stage and an optical fiber interface. Communication between the single HiLEM stages and the overall SoC takes place via optical fibers. All of the needed signals and measurements for the operation of the HiLEM circuit are located on the HiLEM setup itself. Therefore, the higher-level signal processing SoC mainly executes tasks regarding the overall operation and the data collection of the connected HiLEM setup.

IV. SIMULATION RESULTS

To illustrate a possible operating scenario of the HiLEM setup, Fig. 5 shows typical voltage curves for four individual strings u_{G1-4} with solar modules of the

type [8]. The important specifications of the simulated solar modules are shown in Table I. All strings consist of 21 solar modules connected in series. Every string is connected to its own HiLEM input stage. To demonstrate the functional principle of the HiLEM setup, the operational voltages $u_{C1} + u_{C2}$, u_{C2} and the output voltage u_A are also plotted in Fig. 5.

TABLE I: Electrical properties at Standard Test Conditions (STC) from [8]

Nominal power P_{max}	370 W _p
Nominal voltage U_{mp}	34.60 V
Nominal current I_{mp}	10.77 A
Open circuit voltage U_{OC}	41.3 V
short circuit current I_{SC}	11.30 A

The simulation of the shading scenario was performed using a clocking model of the HiLEM topology. For this reason, the simulation results shown in Fig. 5 and Fig. 6 were filtered, since the clock-frequency fractions are not relevant for the desired observation. In addition, the simulation model takes the losses of the semiconductors into account.

String 1 and String 4 are uniformly irradiated with 1000 W/m² and not shaded. String 2 is also uniformly irradiated with 1000 W/m² until time $T1 = 4$ s. Between time $T1$ and time $T2 = 9$ s, shading occurs on one of the 21 solar modules of string 2. From time $T2$ no more shading occurs at string 2. String 3 is irradiated evenly with 1000 W/m² at the beginning. From time point $T1$, three of the 21 solar modules of string 3 are completely shaded causing their bypass diodes to conduct the string current. Table II summarizes the described shading scenario.

TABLE II: Shading scenario for the simulation

String	Irradiation	Shaded Modules	Percentage shaded
1	1000 W/m ²	0	0 %
2	1000 W/m ²	1	100 %
3	1000 W/m ²	3	100 %
4	1000 W/m ²	0	0 %

The HiLEM circuit will operate every string in its individual MPP. To achieve this, the voltage of u_{C1} was set to 150 V and u_{C2} to 600 V. This results in a possible adjustable voltage of the strings from $u_{G,min} \approx 600$ V to $u_{G,max} \approx 750$ V. The output voltage u_A is determined

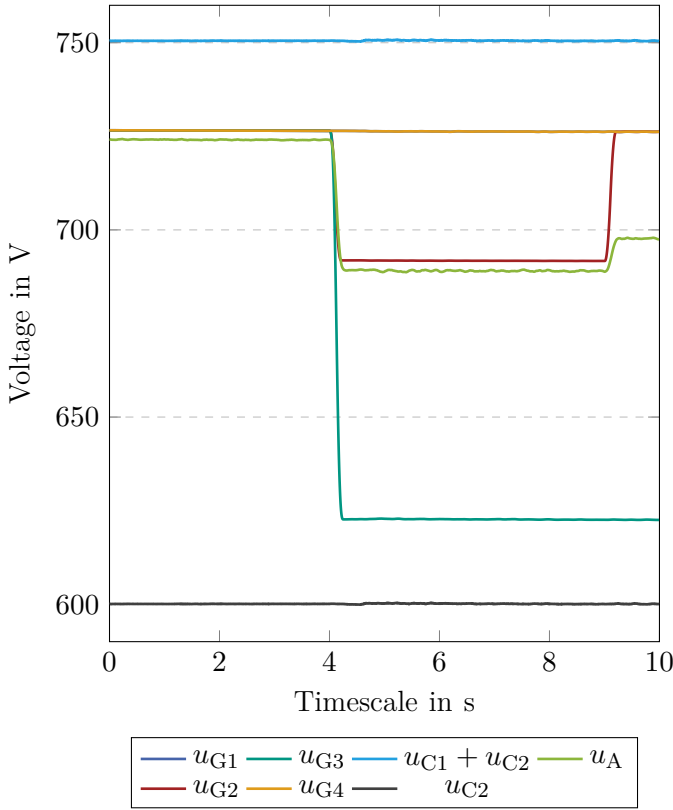


Fig. 5: Simulation results for the voltage curves with the shading scenario

by the input voltages u_{Gx} and the power P_{Gx} of the strings.

Fig. 6 shows the power curves of the individual strings and the corresponding total power, resulting from the simulation. P_1 , P_2 , P_3 and P_4 represent the input power of the respective strings. P_A represents the common output power at the outlet of the HiLEM output stage.

From these values the possible output voltage as well as the output current can be determined. The voltage at the HiLEM output can be considered as a weighted average of the input voltages. Neglecting the losses, the shown example leads from Eq. 9 to

$$u_A \approx u_G = \frac{P_G}{i_G} = \frac{\sum_{x=1}^N u_{Gx} \cdot i_{Gx}}{i_G}. \quad (13)$$

It is obvious from Eq. 13 that the output voltage u_A depends on the individual MPP voltages u_{Gx} and the power of the PV strings P_{Gx} . Boost operation, to achieve a higher voltage level at the output voltage u_A is not possible. For grid feeding operation, attention must be taken to configure the PV strings in such a way that

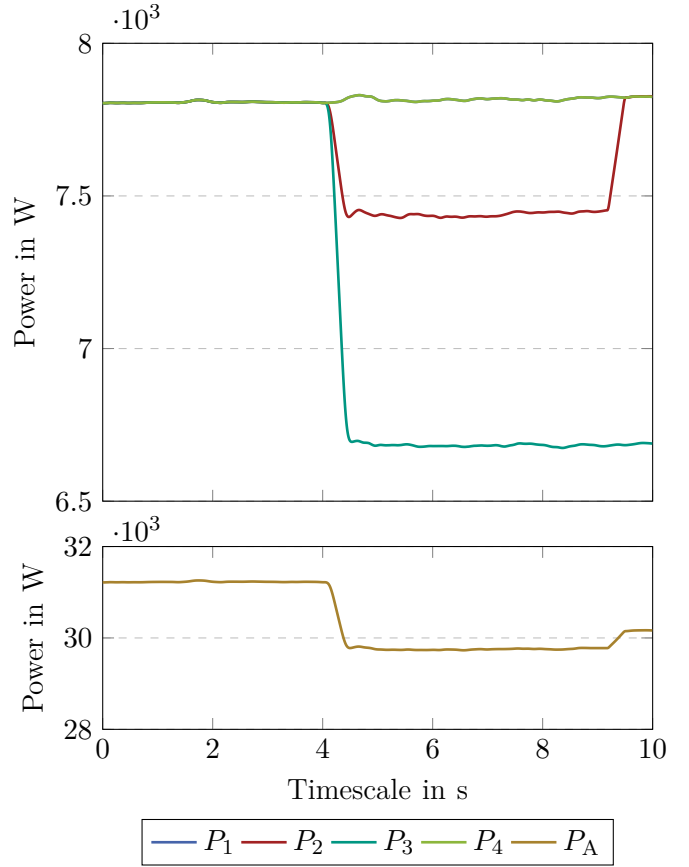


Fig. 6: Simulation results for the resulting power curves with the shading scenario

a suitable voltage level can be achieved. Under certain conditions, operating points can occur at which the voltage level required for the grid feed-in cannot be achieved at the output. In this case, it is necessary to increase the voltage of a string and leave its MPP to meet the required output voltage for grid feed-in.

V. CONCLUSION

This paper addresses the overall design and structure of the first High Efficiency Low Effort MPPT circuit for string-based MPP tracking in large-scale ground-mounted PV systems. First, the need for finely tuned MPP tracking, even in ground-mounted systems, is laid out. Then the current state of technology is described and the advantages of the HiLEM topology as a replacement for combiner boxes in new or existing plants are derived. Furthermore, the possibility to use the HiLEM topology as a replacement for MPPT in conventional string inverters is also discussed and its technical advantages over the other technologies are elaborated.

Moreover, the structure and function of the HiLEM topology is described in detail. The dynamic adjustment of the voltage u_{C1} has significant effects on the overall efficiency. For this reason, further investigations are planned to deal with this question.

An outlook on the hardware setup of the HiLEM prototype is given. In conclusion, the simulation of a possible shading scenario with four strings shows the principle mode of operation. What makes the capabilities of the HiLEM topology apparent.

The detailed hardware design of the HiLEM prototype will follow in a further publication, in which the switching behavior and achievable efficiencies will be discussed in detail.

ACKNOWLEDGEMENT

The authors acknowledge the financial support by the Federal Ministry for Economic Affairs and Climate Action of Germany in the project Solarpark 2.0 (project number 03EE1135A).

REFERENCES

- [1] Federal Republic of Germany, "Erneuerbare-Energien-Gesetz vom 21. Juli 2014 (BGBl. I S. 1066), das zuletzt durch Artikel 6 des Gesetzes vom 4. Januar 2023 (BGBl. 2023 I Nr. 6) geändert worden ist", § 4 Ausbaupfad Abs. 4, 2023.
- [2] Bucciarelli, L. Power loss in photovoltaic arrays due to mismatch in cell characteristics. *Solar Energy*. **23**, pp 277-288, 1979.
- [3] Meinhardt, M., Cramer, G., Burger, B. & Zacharias, P. Multi-string-converter with reduced specific costs and enhanced functionality. *Solar Energy*. **69** pp. 217-227, 2001.
- [4] Gommeringer, M. Neue effiziente und aufwandsarme Schaltungen zum individuellen Maximum Power Point Tracking mehrerer Solarmodulstränge / von Dipl.-Ing. Mario Gommeringer, 2016.
- [5] Gommeringer, M., Schmitt, A., & Kolb, J. "Schaltungsanordnungen und Verfahren zum Abgreifen elektrischer Leistung von mehreren Modulsträngen", Patent application EP2911284A1, published in 2015.
- [6] Brano, V., Orioli, A., Ciulla, G. & Di Gangi, A. An improved five-parameter model for photovoltaic modules. *Solar Energy Materials And Solar Cells*. **94**, 1358-1370, 2010.
- [7] Gommeringer, M., Schmitt, A., Kammerer, F. & Braun, M. "An ultra-efficient maximum power point tracking circuit for photovoltaic inverters" in *2015 41st Annual Conference Of The IEEE Industrial Electronics Society (IECON 2015)*, 2015.
- [8] SOLARWATT, "SOLARWATT Panel vision H 3.0 pure", 370 W_p datasheet, 2022.
- [9] Schwendemann, R., Decker, S., Hiller, M. & Braun, M. A Modular Converter- and Signal-Processing-Platform for Academic Research in the Field of Power Electronics. *2018 International Power Electronics Conference (IPEC-Niigata 2018 -ECCE Asia)*. pp. 3074-3080, 2018.
- [10] Schmitz-Rode, B., Stefanski, L., Schwendemann, R., Decker, S., Mersche, S., Kiehle, P., Himmelmann, P., Liske, A. & Hiller, M. A modular signal processing platform for grid and motor control, HIL and PHIL applications. *2022 International Power Electronics Conference (IPEC-Himeji 2022- ECCE Asia)*, 2022.
- [11] GaN Systems, "Top-side cooled 650 V E-mode GaN transistor", GS66508T datasheet, 2020 [Rev 200402].
- [12] GaN Systems, "Top-side cooled 650 V E-mode GaN transistor", GS66516T datasheet, 2021 [Rev 210727].